FIRENZE 1991

COMPARATIVE STRESS ANALYSIS OF ZERO-CURRENT-SWITCHED QUASI-RESONANT HALFBRIDGE TOPOLOGIES

H.-P. Lüdeke, N. Fröhleke, H. Grotstollen
Institute for power electronics and electrical drives
University of Paderborn, Pohlweg 47–49, D–4790 Paderborn
Phone: 05251-603155 Fax: 05251-603238

Abstract. Device voltage and current stress analysis is performed for zero-current-switched (ZCS) quasi-resonant (QR) halfbrigde power converters. Results are normalized in terms of converter specifications and dimensionless design constraints to permit stress comparison in terms of peak-, rms- and average-quantities for three halfbrigde converter circuits without any detailed design — hence the stress diagrams obtained represent a powerful selection guide and design tool.

Keywords. Quasi–Resonant Converter, Component Stress

1. INTRODUCTION

Looking for new switch topologies for switch-mode power supplies suitable for switching frequencies in the megahertz range without deteriorated efficiency characteristic as compared with today used PWM-converters leads among other topologies to quasi-resonant switches (QRS). QRS, consisting of a power transistor together with one or more diodes for halfwave- (HWO) or fullwave operation (FWO), an inductor and a capacitor – forming a resonant circuit – can turn–on and –off either at zero-current (zero-current-switched quasi-resonant switch, ZCS–QRS) or at zero-voltage (zero-voltage-switched quasi-resonant switch, ZVS–QRS) depending on the arrangement of the resonant elements, minimizing the switching losses. Quasi-resonant converters (QRC) can be derived from PWM-topologies, replacing the active switch by a quasi-resonant one (Liu and Oruganti, 1985).

Analysis of quasi-resonant converters (e.g. Jovanovic et al. 1987, 1988, 1989) reveals that ZVS–QRC are suitable for switching frequencies up to 10MHz significantly decreasing weight and volume of the reactive converter components and improving the dynamic behaviour. Unfortunately ZVS–QRC can not be applied to off-line unclamped (i.e. non bridge-topologies) applications with a wide load range because of excessive transistor voltage stress.

ZCS–QRC can operate 'only' up to 1–2 MHz but can be used for off-line applications with wider load and input voltage range (Jovanovic, Lee and Chen, 1989). Analysis results in dc-conversion ratio diagrams (converter gain diagrams) for halfwave and fullwave operation and design hints considering different design constraints, e.g. to guarantee zero-current switching even at minimum input voltage and maximum load current. To optimize the design and as will be shown in this paper to choose the best converter topology knowledge about the component stress is essential. Three different isolated ZCS–QR halfbridge converters with different location of the resonant capacitor C_P and with respectively without freewheeling diode have been chosen to visualize this.

In the following section the mathematical analysis of the converters in the time domain is shown. General solutions for peak-, average- and rms-quantities are derived. In section 3 the worst-case conditions for the stress quantities are analyzed leading to normalized equations for the maximum peak-, average- and rms-stresses. A comparison of the three converter topologies is given in section 4. General problems with ZCS-QRC are discussed in section 5.

2. DERIVATION OF STRESS QUANTITIES

The analysis of the three ZCS–QR halfbridge converters is performed in the time domain with the following assumptions:

- ideal components,
- constant input voltage,
- large output filter leading to ripplefree filter current. Therefore, the L-C-output filter together with the load can be treated as a constant current sink,
- lossless transformer with negligible magnetizing current. The leakage inductances are taken into consideration only if they can be utilized as a part of the resonant inductance, i.e. if the resonant capacitor is placed on the secondary side of the transformer, see fig. 1b and 1c.

One cycle of opertion of the converters can be described by four topological stages with the equivalent circuits shown in fig. 2 and 3, described in detail for example by Jovanovic, Hopkins and Lee (1987).

Time domain equations for the most important quantities of the three converters are summarized in table 1.

With the results given in table 1 equations for average- and rms-quantities can be derived depending on several design-specific component values of the converter as can be seen below for the average current in switch S1, $I_{S1\,AV}$, as an example. More detailed information is given by Lüdeke (1989) and Fröhleke (1991).

$$I_{S1AV} = \frac{1}{T_S}\left\{\frac{U_i}{2L}\cdot\frac{T_a^2}{2} + \frac{I_a}{N}\cdot T_b + \frac{U_i}{2Z_0}\frac{1}{\omega_0}(1-\cos\omega_0 T_b)\right\} \quad (1)$$

with

T_S		Switching period
$T_a = t_1 - t_0$		Duration of inductor-charging stage
$T_b = t_2 - t_1$		Duration of the resonant stage
$Z_0 = \sqrt{(L/C)}$		Characteristic impedance
$\omega_0 = \sqrt{(LC)}^{-1}$		Resonant frequency.

Inserting the expressions for the time durations T_a, T_b, T_c, T_d of the four stages

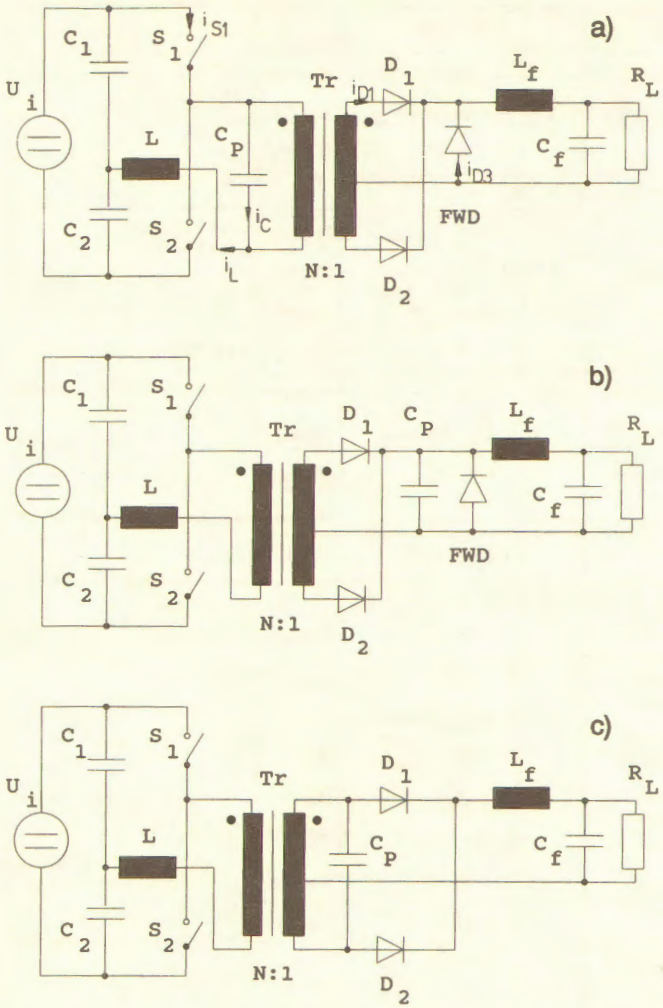

Figure 1: Circuit diagrams of the ideal ZCS–QR halfbridge converters. a) HB, prim, b) HB, sek 1 and c) HB, sek 2.

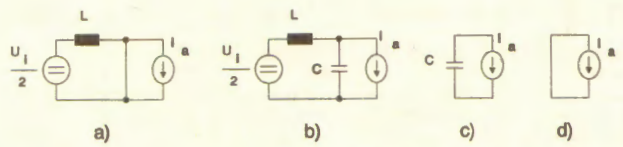

Figure 2: Equivalent circuits of the ideal ZCS–QR halfbridge converters HB, prim and HB, sek 1.
a) inductor-charging stage $[t_o, t_1]$,
b) resonant stage $[t_1, t_2]$,
c) capacitor-discharging stage $[t_2, t_3]$,
d) freewheeling stage $[t_3, t_4]$

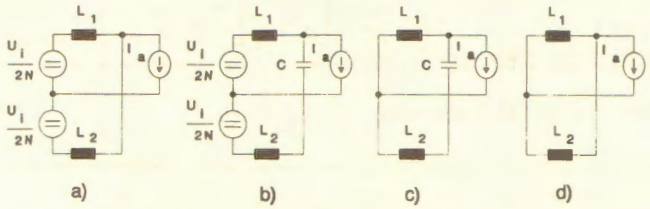

Figure 3: Equivalent circuits of the ideal ZCS–QR halfbridge converter HB, sek 2.
a) inductor-charging stage $[t_o, t_1]$,
b) resonant stage $[t_1, t_2]$,
c) capacitor-discharging stage $[t_2, t_3]$,
d) freewheeling stage $[t_3, t_4]$

$$T_a = \frac{2L}{U_i}\frac{I_a}{N} \tag{2}$$

$$T_b = \arcsin\left(-\frac{I_a}{N}\frac{2Z_0}{U_i}\right)\Big/\omega_0 \stackrel{!}{=} \frac{\alpha}{\omega_0} \tag{3}$$

$$T_c = u_C(t_2)\frac{CN}{I_a} = \frac{U_i}{2}(1-\cos\omega_0 T_b)\,\frac{CN}{I_a} \tag{4}$$

$$T_d = T_S - T_a - T_b - T_c \quad \underbrace{(-\frac{T_S}{2})}_{\text{dep. on periodicity}} \tag{5}$$

and defining the following design constraints

- normalized switching frequency $f_n = f_S/f_0$ (switching to resonant frequency)
- converter gain $M = (U_a \cdot N)\ /\ (U_i/2)$ (output to input voltage reflected to the primary side)
- normalized load resistance $Q = (R_L \cdot N^2)\ /\ Z_0$ (load resistance to characteristic tank impedance reflected to the primary side)

and abbreviations

$$\alpha = \arcsin\left(-\frac{M}{Q}\right)$$

$$\cos\alpha = \mp\sqrt{1-\left(\frac{M}{Q}\right)^2} \qquad -: \text{HWO}\ ;\ +: \text{FWO}$$

$$sin2\alpha = \pm 2\,\frac{M}{Q}\cdot\sqrt{1-\left(\frac{M}{Q}\right)^2} \qquad +: \text{HWO}\ ;\ -: \text{FWO}$$

normalized equations are obtained for peak-, average- and rms-quantities only in terms of the input voltage, the output current, the normalized frequency and the dimensionless ratio Q/M defined as ζ,

$$\frac{I_{S1AV}}{I_a/N} = \frac{f_n}{2\pi}\left\{\frac{1}{2}\frac{M}{Q} + \arcsin\left(-\frac{M}{Q}\right) + \frac{Q}{M}\left(1 \pm \sqrt{1-\left(\frac{M}{Q}\right)^2}\right)\right\} \tag{6}$$

where the correct sign of $\pm$ depends on whether the converter operates in halfwave (HWO) or fullwave (FWO) mode. The base quantities for the normalization are I_a and $U_i/2$ respectively I_a/N and $U_i/(2N)$ for quantities on the primary side.

3. MAXIMUM STRESS QUANTITIES

Design constraint ζ defined as ratio of normalized load resistance to converter gain also represents the ratio of peak resonant tank current to constant output current (reflected to the primary side). If line and load variations are considered, i.e. $Q_{min} \le Q \le Q_{max}$ and $M_{min} \le M \le M_{max}$, the converters have to be designed for the worst-case, i.e. full load (Q_{min}) and low input voltage (M_{max}) to achieve zero-current-switching for the whole line and load range. For ζ this leads to

$$\zeta = \zeta_{ZCS} = \frac{Q_{min}}{M_{max}} \stackrel{!}{\ge} 1.0 \tag{7}$$

as has been shown by Lotfi (1988). On the other hand large values of ζ increase the resonant tank current amplitude and thereby the conduction losses especially of the quasi-resonant switch. Hence, to minimize the conduction losses and to satisfy the above mentio-

	HB, prim	*HB, sek1*	*HB, sek2*	
i_{S1}	$\frac{U_i}{2L} \cdot t$	$\frac{U_i}{2N^2L} \cdot t$	$2\frac{U_i}{2N^2L_1} \cdot t$	$[t_0, t_1]$
	$\frac{U_i}{2Z_0} \sin\omega_0 t + \frac{I_a}{N}$	$\frac{U_i}{2Z_0N^2} \sin\omega_0 t + \frac{I_a}{N}$	$4\frac{U_i}{2Z_0N^2} \sin\omega_0 t + \frac{I_a}{N}$	$[t_1, t_2]$
	0	0	0	$[t_2, 2t_4]$
i_{S2}	*analogous at interval* $[t_4, 3t_4]$			
u_C	0	0	0	$[t_0, t_1]$
	$\pm\left[\frac{U_i}{2}(1 - cos\omega_0 t)\right]$	$\frac{U_i}{2N}(1 - cos\omega_0 t)$	$\pm\left[2\frac{U_i}{2N}(1 - cos\omega_0 t)\right]$	$[t_1, t_2]$
	$\pm\left[u_C(t_2) - \frac{I_a}{NC} \cdot t\right]$	$u_C(t_2) - \frac{I_a}{C} \cdot t$	$\pm\left[u_C(t_2) - \frac{I_a}{2C} \cdot t\right]$	$[t_2, t_3]$
	0	0	0	$[t_3, t_4]$
i_C	0	0	0	$[t_0, t_1]$
	$\pm\left[\frac{U_i}{2Z_0} \sin\omega_0 t\right]$	$\frac{U_i}{2NZ_0} \sin\omega_0 t$	$\pm\left[2\frac{U_i}{2NZ_0} \sin\omega_0 t\right]$	$[t_1, t_2]$
	$\pm\left[-\frac{I_a}{N}\right]$	$-I_a$	$\pm\left[-\frac{I_a}{2}\right]$	$[t_2, t_3]$
	0	0	0	$[t_3, t_4]$
i_L	$\pm\left[\frac{U_i}{2L} \cdot t\right]$	$\pm\left[\frac{U_i}{2N^2L} \cdot t\right]$	$\pm 2\frac{U_i}{2N^2L_1} \cdot t$	$[t_0, t_1]$
	$\pm\left[\frac{U_i}{2Z_0} \sin\omega_0 t + \frac{I_a}{N}\right]$	$\pm\left[\frac{U_i}{2N^2Z_0} \sin\omega_0 t + \frac{I_a}{N}\right]$	$\pm\left[4\frac{U_i}{2N^2Z_0} \sin\omega_0 t + \frac{I_a}{N}\right]$	$[t_1, t_2]$
	0	0	0	$[t_2, t_4]$
i_{L1}	*corresponding to*	*corresponding to*	$\frac{I_a}{2} + \frac{U_i}{2NL_1} \cdot t$	$[t_0, t_1]$
			$I_a + 2\frac{U_i}{2NZ_0} \sin\omega_0 t$	$[t_1, t_2]$
	$i_{D1}(t)$	$i_{D1}(t)$	$\frac{I_a}{2}$	$[t_2, t_4]$
			$\frac{I_a}{2} - \frac{U_i}{2NL_1} \cdot t$	$[t_4, t_5]$
			$-2\frac{U_i}{2NZ_0} \sin\omega_0 t$	$[t_5, t_6]$
			$\frac{I_a}{2}$	$[t_6, 2t_4]$
i_{D1}	$\frac{U_i}{2L} \cdot N \cdot t$	$\frac{U_i}{2NL} \cdot t$	$\frac{I_a}{2} \pm \frac{U_i}{2NL_1} \cdot t$	$[t_0, t_1]$
	I_a	$I_a + \frac{U_i}{2NZ_0} \sin\omega_0 t$	$\frac{I_a}{2} \pm \frac{I_a}{2}$	$[t_1, t_3]$
	0	0	$\frac{I_a}{2}$	$[t_3, t_4]$
	0	0	*analogous, '−' valid*	$[t_4, 2t_4]$
i_{D2}	*analogous at interval* $[t_4, 3t_4]$			
u_{D2}	0	$\frac{U_i}{2N}$	0	$[t_0, t_1]$
	$2\frac{U_i}{2N}(1 - \cos\omega_0 t)$	$\frac{U_i}{2N}(2 - \cos\omega_0 t)$	$2\frac{U_i}{2N}(1 - \cos\omega_0 t)$	$[t_1, t_2]$
	$\frac{2}{N}\left[u_C(t_2) - \frac{I_a}{NC} \cdot t\right]$	0	$u_C(t_2) - \frac{I_a}{2C} \cdot t$	$[t_2, t_3]$
	0	0	0	$[t_3, 2t_4]$
u_{D1}	*analogous at interval* $[t_4, 3t_4]$			
i_{D3}	$I_a - \frac{U_i}{2L} \cdot N \cdot t$	$I_a - \frac{U_i}{2N^2L} \cdot t$		$[0, t_1]$
	0	0		$[t_1, t_3]$
	I_a	I_a		$[t_3, t_4]$
u_{D3}	0	0		$[t_0, t_1]$
	$\frac{U_i}{2N}(1 - \cos\omega_0 t)$	$\frac{U_i}{2N}(1 - \cos\omega_0 t)$		$[t_1, t_2]$
	$\frac{1}{N}\left[u_C(t_2) - \frac{I_a}{NC} t\right]$	$u_C(t_2) - \frac{I_a}{C} t$		$[t_2, t_3]$
	0	0		$[t_3, t_4]$

+ : S1 on − : S2 on

Table 1: Time domain equations for ZCS–QR halfbridges

	HB,prim	HB,sek1	HB,sek2
$\left(\frac{I_{S1AV}}{I_a/N}\right)_{max}$	$\frac{f_S}{f_o}\frac{1}{2\pi}\left\{\frac{1}{2}\frac{M_{max}}{Q_{min}}+\arcsin\left(-\frac{M_{max}}{Q_{min}}\right)+\frac{Q_{min}}{M_{max}}\left(1\pm\sqrt{1-\left(\frac{M_{max}}{Q_{min}}\right)^2}\right)\right\}$	$\frac{f_S}{f_o}\frac{1}{2\pi}\left\{\frac{1}{2}\frac{M_{max}}{Q_{min}}+\arcsin\left(-\frac{M_{max}}{Q_{min}}\right)+\frac{Q_{min}}{M_{max}}\left(1\pm\sqrt{1-\left(\frac{M_{max}}{Q_{min}}\right)^2}\right)\right\}$	$\frac{f_S}{f_o}\frac{1}{2\pi}\left\{\frac{1}{2}\frac{M_{max}}{4Q_{min}}+\arcsin\left(-\frac{M_{max}}{4Q_{min}}\right)+\frac{4Q_{min}}{M_{max}}\left(1\pm\sqrt{1-\left(\frac{M_{max}}{4Q_{min}}\right)^2}\right)\right\}$
$\left(\frac{I_{S1RMS}}{I_a/N}\right)_{max}$	$\left\{\frac{f_S}{f_o}\frac{1}{2\pi}\left[\frac{1}{3}\frac{M_{max}}{Q_{min}}+\frac{1}{2}\left(\frac{Q_{min}}{M_{max}}\right)^2\arcsin\left(-\frac{M_{max}}{Q_{min}}\right)\mp\frac{1}{2}\frac{Q_{min}}{M_{max}}\sqrt{1-\left(\frac{M_{max}}{Q_{min}}\right)^2}+\arcsin\left(-\frac{M_{max}}{Q_{min}}\right)+2\frac{Q_{min}}{M_{max}}\left(1\pm\sqrt{1-\left(\frac{M_{max}}{Q_{min}}\right)^2}\right)\right]\right\}^{1/2}$	$\left\{\frac{f_S}{f_o}\frac{1}{2\pi}\left[\frac{1}{3}\frac{M_{max}}{Q_{min}}+\frac{1}{2}\left(\frac{Q_{min}}{M_{max}}\right)^2\cdot\arcsin\left(-\frac{M_{max}}{Q_{min}}\right)\mp\frac{1}{2}\frac{Q_{min}}{M_{max}}\sqrt{1-\left(\frac{M_{max}}{Q_{min}}\right)^2}+\arcsin\left(-\frac{M_{max}}{Q_{min}}\right)+2\frac{Q_{min}}{M_{max}}\left(1\pm\sqrt{1-\left(\frac{M_{max}}{Q_{min}}\right)^2}\right)\right]\right\}^{1/2}$	$\left\{\frac{f_S}{f_o}\frac{1}{2\pi}\left[\frac{1}{3}\frac{M_{max}}{4Q_{min}}+\frac{1}{2}\left(\frac{4Q_{min}}{M_{max}}\right)^2\cdot\arcsin\left(-\frac{M_{max}}{4Q_{min}}\right)\mp\frac{1}{2}\frac{4Q_{min}}{M_{max}}\sqrt{1-\left(\frac{M_{max}}{4Q_{min}}\right)^2}+\arcsin\left(-\frac{M_{max}}{4Q_{min}}\right)+2\frac{4Q_{min}}{M_{max}}\left(1\pm\sqrt{1-\left(\frac{M_{max}}{4Q_{min}}\right)^2}\right)\right]\right\}^{1/2}$
$\left(\frac{I_{LRMS}}{I_a/N}\right)_{max}$	$\left\{\underbrace{\frac{f_S}{f_o}\frac{1}{\pi}\left[\frac{1}{3}\frac{M_{max}}{Q_{min}}+\dots\right]}_{\text{siehe } I_{S1RMS}}\right\}^{1/2}$	$\left\{\underbrace{\frac{f_S}{f_o}\frac{1}{\pi}\left[\frac{1}{3}\frac{M_{max}}{Q_{min}}+\dots\right]}_{\text{siehe } I_{S1RMS}}\right\}^{1/2}$	$\left\{\underbrace{\frac{f_S}{f_o}\frac{1}{\pi}\left[\frac{1}{3}\frac{M_{max}}{Q_{min}}+\dots\right]}_{\text{siehe } I_{S1RMS}}\right\}^{1/2}$
$\left(\frac{I_{CAV}}{I_a}\right)_{max}$	0	0	0
$\left(\frac{I_{CRMS}}{I_a/N}\right)_{max}$ ① $\left(\frac{I_{CRMS}}{I_a}\right)_{max}$ ②	$\left\{\frac{f_S}{f_o}\frac{1}{\pi}\left[\frac{1}{2}\left(\frac{Q_{min}}{M_{max}}\right)^2\arcsin\left(-\frac{M_{max}}{Q_{min}}\right)\mp\frac{1}{2}\frac{Q_{min}}{M_{max}}\sqrt{1-\left(\frac{M_{max}}{Q_{min}}\right)^2}+\frac{Q_{min}}{M_{max}}\left(1\pm\sqrt{1-\left(\frac{M_{max}}{Q_{min}}\right)^2}\right)\right]\right\}^{1/2}$ ①	$\left\{\frac{f_S}{f_o}\frac{1}{\pi}\left[\frac{1}{2}\left(\frac{Q_{min}}{M_{max}}\right)^2\cdot\arcsin\left(-\frac{M_{max}}{Q_{min}}\right)\mp\frac{1}{2}\frac{Q_{min}}{M_{max}}\sqrt{1-\left(\frac{M_{max}}{Q_{min}}\right)^2}+\frac{Q_{min}}{M_{max}}\left(1\pm\sqrt{1-\left(\frac{M_{max}}{Q_{min}}\right)^2}\right)\right]\right\}^{1/2}$ ②	$2\left\{\frac{f_S}{f_o}\frac{1}{\pi}\left[\frac{1}{2}\left(\frac{4Q_{min}}{M_{max}}\right)^2\cdot\arcsin\left(-\frac{M_{max}}{4Q_{min}}\right)\mp\frac{1}{2}\frac{4Q_{min}}{M_{max}}\sqrt{1-\left(\frac{M_{max}}{4Q_{min}}\right)^2}+\frac{4Q_{min}}{M_{max}}\left(1\pm\sqrt{1-\left(\frac{M_{max}}{4Q_{min}}\right)^2}\right)\right]\right\}^{1/2}$ ②
$\left(\frac{I_{D1AV}}{I_a}\right)_{max}$	$\frac{f_S}{f_o}\frac{1}{2\pi}\left\{\frac{1}{2}\frac{M_{max}}{Q_{min}}+\arcsin\left(-\frac{M_{max}}{Q_{min}}\right)+\frac{Q_{min}}{M_{max}}\left(1\pm\sqrt{1-\left(\frac{M_{max}}{Q_{min}}\right)^2}\right)\right\}$	$\frac{f_S}{f_o}\frac{1}{2\pi}\left\{\frac{1}{2}\frac{M_{max}}{Q_{min}}+\arcsin\left(-\frac{M_{max}}{Q_{min}}\right)+\frac{Q_{min}}{M_{max}}\left(1\pm\sqrt{1-\left(\frac{M_{max}}{Q_{min}}\right)^2}\right)\right\}$	1/2
$\left(\frac{I_{D1RMS}}{I_a}\right)_{max}$	$\left\{\frac{f_S}{f_o}\frac{1}{2\pi}\left[\frac{1}{3}\frac{M_{max}}{Q_{min}}+\arcsin\left(-\frac{M_{max}}{Q_{min}}\right)+\frac{Q_{min}}{M_{max}}\left(1\pm\sqrt{1-\left(\frac{M_{max}}{Q_{min}}\right)^2}\right)\right]\right\}^{1/2}$	$\left\{\frac{f_S}{f_o}\frac{1}{2\pi}\left[\frac{1}{3}\frac{M_{max}}{Q_{min}}+\frac{1}{2}\left(\frac{Q_{min}}{M_{max}}\right)^2\arcsin\left(-\frac{M_{max}}{Q_{min}}\right)\mp\frac{1}{2}\frac{Q_{min}}{M_{max}}\sqrt{1-\left(\frac{M_{max}}{Q_{min}}\right)^2}+\arcsin\left(-\frac{M_{max}}{Q_{min}}\right)+2\frac{Q_{min}}{M_{max}}\left(1\pm\sqrt{1-\left(\frac{M_{max}}{Q_{min}}\right)^2}\right)\right]\right\}^{1/2}$	$\frac{1}{2}\left\{1+\frac{f_s}{f_o}\frac{1}{2\pi}\left[\frac{1}{3}\frac{M_{max}}{4Q_{min}}+\arcsin\left(-\frac{M_{max}}{4Q_{min}}\right)+\frac{4Q_{min}}{M_{max}}\left(1\pm\sqrt{1-\left(\frac{M_{max}}{4Q_{min}}\right)^2}\right)\right]\right\}^{1/2}$
$\left(\frac{I_{D3AV}}{I_a}\right)_{max}$	$\frac{f_S}{f_o}\frac{1}{\pi}\left\{\pi\frac{f_o}{f_S}-\frac{1}{2}\frac{M_{min}}{Q_{min}}-\arcsin\left(-\frac{M_{min}}{Q_{min}}\right)-\frac{Q_{min}}{M_{min}}\left(1\pm\sqrt{1-\left(\frac{M_{min}}{Q_{min}}\right)^2}\right)\right\}$	$\frac{f_S}{f_o}\frac{1}{\pi}\left\{\pi\frac{f_o}{f_S}-\frac{1}{2}\frac{M_{min}}{Q_{min}}-\arcsin\left(-\frac{M_{min}}{Q_{min}}\right)-\frac{Q_{min}}{M_{min}}\left(1\pm\sqrt{1-\left(\frac{M_{min}}{Q_{min}}\right)^2}\right)\right\}$	
$\left(\frac{I_{D3RMS}}{I_a}\right)_{max}$	$\left\{\frac{f_S}{f_o}\frac{1}{\pi}\left[\pi\frac{f_o}{f_S}-\frac{2}{3}\frac{M_{min}}{Q_{min}}-\arcsin\left(-\frac{M_{min}}{Q_{min}}\right)-\frac{Q_{min}}{M_{min}}\left(1\pm\sqrt{1-\left(\frac{M_{min}}{Q_{min}}\right)^2}\right)\right]\right\}^{1/2}$	$\left\{\frac{f_S}{f_o}\frac{1}{\pi}\left[\pi\frac{f_o}{f_S}-\frac{2}{3}\frac{M_{min}}{Q_{min}}-\arcsin\left(-\frac{M_{min}}{Q_{min}}\right)-\frac{Q_{min}}{M_{min}}\left(1\pm\sqrt{1-\left(\frac{M_{min}}{Q_{min}}\right)^2}\right)\right]\right\}^{1/2}$	
$\left(\frac{U_{CRMS}}{U_i/2}\right)_{max}$ ① $\left(\frac{U_{CRMS}}{U_i/2N}\right)_{max}$ ②	$\left\{\frac{f_S}{f_o}\frac{1}{\pi}\left[1{,}5\cdot\arcsin\left(-\frac{M_{min}}{Q_{max}}\right)+2\frac{M_{min}}{Q_{max}}\pm\frac{1}{2}\frac{M_{min}}{Q_{max}}\sqrt{1-\left(\frac{M_{min}}{Q_{max}}\right)^2}+\frac{1}{3}\frac{Q_{max}}{M_{min}}\left(1\pm\sqrt{1-\left(\frac{M_{min}}{Q_{max}}\right)^2}\right)^3\right]\right\}^{1/2}$ ①	$\left\{\frac{f_S}{f_o}\frac{1}{\pi}\left[1{,}5\cdot\arcsin\left(-\frac{M_{min}}{Q_{max}}\right)+2\frac{M_{min}}{Q_{max}}\pm\frac{1}{2}\frac{M_{min}}{Q_{max}}\sqrt{1-\left(\frac{M_{min}}{Q_{max}}\right)^2}+\frac{1}{3}\frac{Q_{max}}{M_{min}}\left(1\pm\sqrt{1-\left(\frac{M_{min}}{Q_{max}}\right)^2}\right)^3\right]\right\}^{1/2}$ ②	$2\cdot\left\{\frac{f_S}{f_o}\frac{1}{\pi}\left[1{,}5\cdot\arcsin\left(-\frac{M_{min}}{4Q_{max}}\right)+2\frac{M_{min}}{4Q_{max}}\pm\frac{1}{2}\frac{M_{min}}{4Q_{max}}\sqrt{1-\left(\frac{M_{min}}{4Q_{max}}\right)^2}+\frac{1}{3}\frac{4Q_{max}}{M_{min}}\left(1\pm\sqrt{1-\left(\frac{M_{min}}{4Q_{max}}\right)^2}\right)^3\right]\right\}^{1/2}$ ②
	$\zeta_C=\frac{Q_{min}}{M_{max}}\ge 1.0$	$\zeta_C=\frac{Q_{min}}{M_{max}}\ge 1.0$	$\zeta_C=\frac{4Q_{min}}{M_{max}}\ge 1.0$

Table 2: Normalized equations for maximum average- and rms-quantities

ned constraint ζ should be as close to 1.0 as possible. For higher input voltages values of 1.05...1.3 for ζ seem to be appropriated. For lower input voltages $\zeta \approx 1.3$ has to be chosen because of the more accentuated damping influences of the parasitic elements in the resonant tank circuit.

It has been found that Q_{min} and M_{max} represent just the worst-case for the rms- and average-current values except of the current in the freewheeling diode. Its maximum rms- and average current values appear at $U_{i\,max}$ and $I_{a\,max}$, i.e. at Q_{min} and M_{min}, because under these conditions the duration of the freewheeling stage becomes maximum. The maximum rms- and average quantities for the three converters in normalized form are summarized in table 2. The maximum peak stresses appear at full load and high input voltage, i.e. at Q_{min} and M_{min}, and are independent of the switching frequency. The maximum peak stress quantities in normalized form are shown in table 3.

	$HB, prim$	$HB, sek1$	$HB, sek2$
$\left(\frac{i_{S1}}{I_a/N}\right)_{max}$	$1+\frac{Q_{min}}{M_{min}}$	$1+\frac{Q_{min}}{M_{min}}$	$1+4\frac{Q_{min}}{M_{min}}$
$\left(\frac{u_{DS}}{U_i/2}\right)_{max}$	2	2	2
$\left(\frac{u_C}{U_i/2}\right)_{max}$	2	2 *	4 *
$\left(\frac{i_C}{I_a/N}\right)_{max}$	$\frac{Q_{min}}{M_{min}}$	$\frac{Q_{min}}{M_{min}}$ **	$2\frac{Q_{min}}{M_{min}}$ **
$\left(\frac{u_{D1,2}}{U_i/2N}\right)_{max}$	4	3	4
$\left(\frac{i_{D1,2}}{I_a}\right)_{max}$	1	$1+\frac{Q_{min}}{M_{min}}$	1
$\left(\frac{u_{D3}}{U_i/2N}\right)_{max}$	2	2	/
$\left(\frac{i_{D3}}{I_a}\right)_{max}$	1	1	/

* u_c reflected to the primary side

** i_c reflected to the primary side

Table 3: Normalized maximum ratings of ZCS–QR–halfbridges

The above derived equations for the stress quantities lead to stress diagrams – normalized average- or rms-stress quantities versus normalized switching frequency with Q/M as parameter – for each converter offering the feasibility to compare different converter topologies not only in terms of the peak stresses as has been done by Lotfi (1988) and to choose an optimum input and load range without any detailed design. Figure 4 shows the stress diagrams for different quantities of HB, prim.

4. COMPARISON OF CONVERTER TOPOLOGIES

With the results of the stress analysis, the main advantages resp. disadvantages of the three converter topologies can be pointed out.

HB, prim

On one hand, by placing the resonant capacitor C_P on the primary side the transformer leakage inductances cannot be utilized as resonant elements. Therefore the transformer has to be designed as for a PWM-converter, i.e. with minimum leakage inductances to reduce parasitic oscillations on the secondary side. On the other hand, for applications with low output voltage and high output current C_P has to carry only a relative low ac-current compared with the converters with secondary side resonance (HB,sek 1 and sek 2) and the transformer has to be designed for much less reactive power reducing its volume and weight.

HB, sek 1 and HB, sek 2

The converter variants HB, sek 1 and HB, sek 2 utilize the transformer leakage inductances as resonant inductance eliminating the problem of parasitic oscillations caused by the leakage inductances and the parasitic capacitances of the rectifier diodes. The transformer has to be designed for a higher volt-ampere product compared with HB, prim because it is part of the resonant circuit.
In HB, sek 1 the rectifier diodes D1, D2, which are also located in the resonant circuit, cause additional losses. This converter can only operate in halfwave mode because D1 and D2 prevent bidirectional current flow in the resonant tank circuit. Yet, the design of the quasi-resonant switches is quite simple because discrete blocking diodes are not necessary (see Jovanovic, Hopkins and Lee, 1989).

5. GENERAL PROBLEMS WITH ZCS-QRC

The analysis of ZCS-QRC reveals the following restrictions for the application of these converters:

- They are not suitable for wide input voltage range, if a good efficiency characteristic is required.
- High input voltages cause significant discharging losses of the parasitic transistor output capacitance C_{OSS} at turn-on of the transistor proportional to the square of input voltage ($P_l = 0.5\,C_{OSS}\,U_i{}^2\,f_S$).
- A small switching frequency range Δf_S can only be attained by fullwave operation of the converter leading to a quasi-resonant switch with at least two diodes, increasing component count and conduction losses, while it causes parasitic oscillations at turn-off of the antiparallel diode because of its reverse recovery characteristic (see Jovanovic, Hopkins and Lee, 1989).

Most of these restrictions and drawbacks can be overcome, if resonant converters, e.g. series-parallel-loaded resonant converters, operating above resonance are applied (see Lüdeke, Fröhleke and Grotstollen in this conference record).

6. CONCLUSIONS

A stress analysis for zero-current-switched quasi-resonant converters has been performed permitting the comparison of different converter topologies in terms of peak-, rms- and average-stress quantities. The analysis has been applied to three different ZCS-QR-halfbridge converters revealing advantages and disadvantages of each topology.
According to experience, damping in the resonant tank circuit and voltage drops of the diodes lead to deviations for example of the waveforms in the resonant tank circuit and of the converter gain from the results, obtained by the ideal analysis. Consequences for ZCS-QRC operating in fullwave mode are much more significant than for halfwave operation, because damping prevents, that the resonant tank current reaches its theoretical amplitudes leading to an earlier loss of zero-current-switching. Expansion of the analysis to the non-ideal case has to be done in the future.

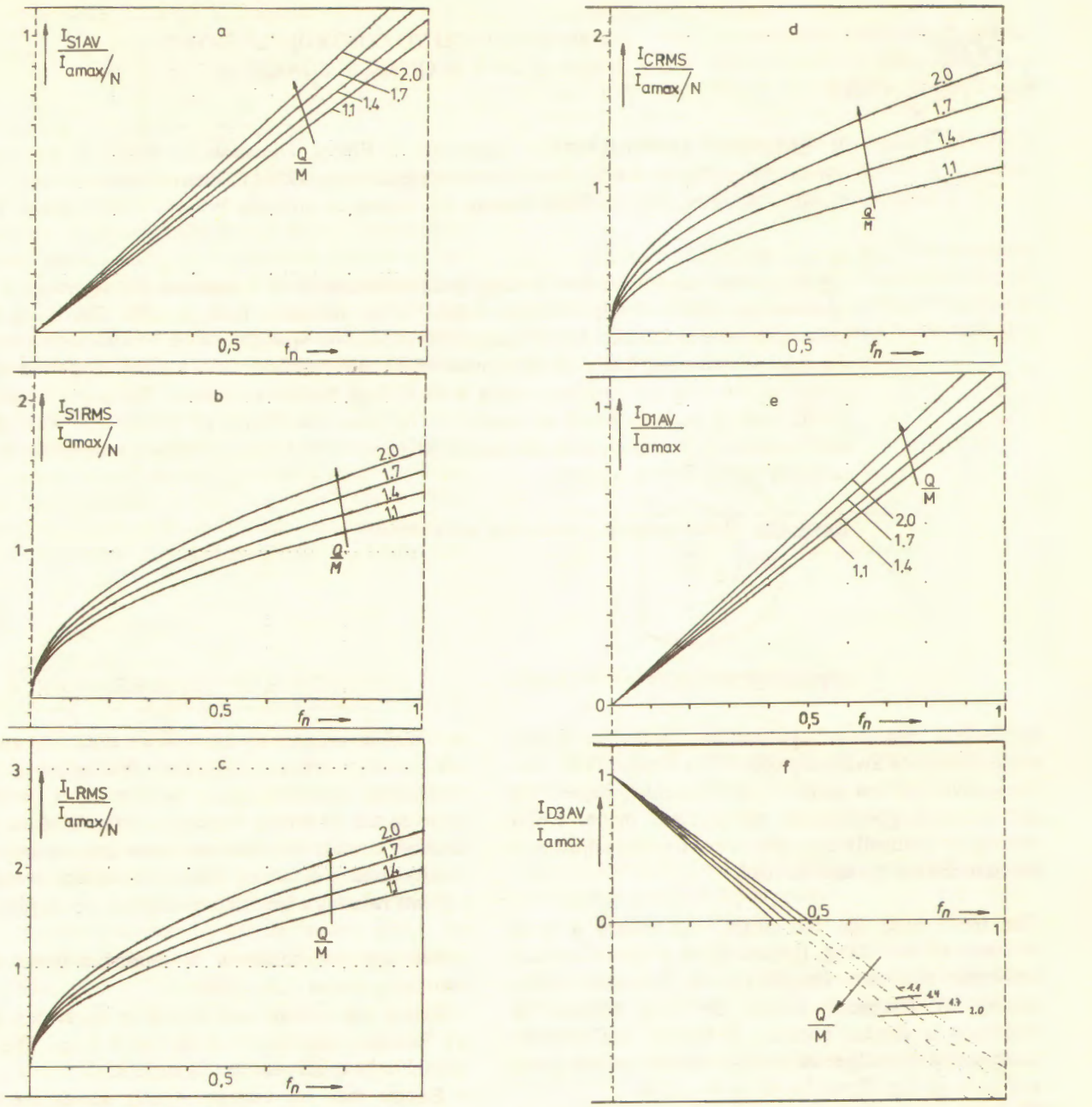

Figure 4: Stress diagrams for different converter quantities for HB, prim as an example
a) Normalized AV- and b) RMS-transistor current
c) Normalized RMS-resonant inductor current
d) Normalized RMS-resonant capacitor current
e) Normalized AV-current in a rectifier diode
f) Normalized AV-current in the freewheeling diode (negativ values are of no practical meaning because the diode never conducts)

REFERENCES

1) **Fröhleke N.** (1991) "Topologien und Schalterkonzepte für Schaltnetzteile hoher Leistung bei geringer Ausgangsspannung". Ph. D. Dissertation, University of Paderborn.

2) **Jovanovic M., Hopkins D. and Lee F.C.** (1987). "Design aspects for high-frequency off-line quasi-resonant converters". High Frequency Power Electronics Conference (HFPC) Record, pp. 83-87.

3) **Jovanovic M., Hopkins D. and Lee F.C.** (1989). "Evaluation and design of megahertz-frequency off-line zero-current-switched quasi-resonant converters". IEEE Transactions on Power Electronics, Vol. 4, No. 1, pp. 136-145.

4) **Jovanovic M., Lee F.C. and Chen D.Y.** (1989). "A zero-current-switched off-line quasi-resonant converter with reduced frequency range: Analysis, Design and experimental results". IEEE Transactions on Power Electronics, Vol. 4, No. 2, pp. 215-224.

5) **Liu K.H., Oruganti R. and Lee F.C.** (1985). "Resonant switches – topologies and characteristics". Power Electronics Specialists Conference (PESC) Record, pp. 106-116.

6) **Lotfi A., Vorperian V. and Lee F.C.** (1988). "Comparison of stresses in quasi-resonant and pulse-width-modulated converters". IEEE Power Electronics Specialists Conference (PESC) Record, pp. 591-599.

7) **Lüdeke H.-P.** (1989). "Vergleichende Analyse von Resonanzkonvertern für hohe Ausgangsleistung bei geringer Ausgangsspannung". M.S. Thesis, University of Paderborn.